Summarizing Large Scale 3D Point Cloud for Navigation Tasks

Imeen Ben Salah, Sebastien Kramm, Cédric Demonceaux, Pascal Vasseur

Summarizing Large Scale 3D Point Cloud for Navigation Tasks

Imeen Ben Salah*, Sébastien Kramm*, Cédric Demonceaux† and Pascal Vasseur*
*Laboratoire d'Informatique, de Traitement de l'Information et des Systèmes
Normandie Univ, UNIROUEN, UNIHAVRE, INSA Rouen, LITIS, 76000 Rouen, France
†Laboratoire LE2I FRE 2005, CNRS, Arts et Métiers, Univ. Bourgogne Franche-Comté

***Abstract*—Democratization of 3D sensor devices makes 3D maps building easier especially in long term mapping and autonomous navigation. In this paper we present a new method for summarizing a 3D map (dense cloud of 3D points). This method aims to extract a summary map facilitating the use of this map by navigation systems with limited resources (smartphones, cars, robots...). This Vision-based summarizing process is applied in a fully automatic way using the photometric, geometric and semantic information of the studied environment.**

I. Introduction

Last years, the introduction of High-Definition (HD) and semantic maps has made a great participation in the large commercial success of navigation and mapping products and also in the enhancement of data fusion based localization algorithms. Several digital map suppliers like TomTom and HERE are now providing HD maps with higher navigation accuracy, especially in challenging urban environments. On the one hand, these HD maps provide more detailed representation of the environment even within large-scale 3D point cloud data. On the other hand, they require a high processing capacity with severe time constraints as well as a large storage requirement. Hence the need to find a new method to summarize these maps in order to reduce the required resources (computation / memory) to run the intelligent transportation systems while preserving the essential navigation information (saliency pixels, important nodes, etc.).

II. PREVIOUS WORKS

In some navigation tasks, setting a full-size map on a mobile device (car, robot, etc.) poses several difficulties. Appearance-based navigation methods are based on global features like color, histogram or local features like points. To simplify the process of appearance-based navigation, a selection process is applied to select the key/reference features in the environment. In the visual memory approach a set of relevant and distinctive areas (images) are acquired and used during navigation by comparing it to the current position. This approach could serve to produce a compact summary of a map [9], [15], [16]. In the work of Cobzas [3], an example of panoramic memory of images is created by combining the acquired images with the depth information extracted from a laser scanner. In this image database, only the essential information to the navigation process will be retained [2]. This allows to obtain homogeneous results with the same properties (precision, convergence, robustness,...) as the original global map. In order to build this image database, some techniques have been developed in order to guarantee the maximum efficiency in the choice of useful information. A spherical representation has been proposed by M. Meilland *et al.* [5], [13], [14]. This spherical representation is build by merging different images acquired by a set of cameras with the depth information extracted from a laser scanner. In this representation, all the information necessary for localization is present and compacted in a single sphere, thus avoiding the mapping of areas unnecessary to navigation [14]. We build upon this idea in this paper, as this approach is promising. Methods based on Bag of Words (BoW) are widely used for localization. BoW methods can efficiently represent a huge amount of data using the occurrences of several visual vocabulary. By applying hierarchical dictionary to the visual navigation problem [19], BoW methods proved a high scalability and accuracy in vision-based localization and mapping processes. The huge number of 3D points in HD maps makes point cloud compression algorithms essential for efficient storage and transmission. Over the past decade, several compression approaches have been proposed in literature. Some of them employ special data structures such as octree [4] [6] for progressive encoding of point clouds. Schnabel *et al.* [17] propose a prediction scheme to achieve the compression using the octree approach. A novel compression method has been proposed in [10] to code only the spatial and temporal differences within an octree structure. Jae-Kyun *et al.* [1] proposed a geometry compression algorithm for large scale point cloud to encode radial distances in a range image. Several approaches based on feature selection to summarize a map for localization purposes were presented in [23], [24], [25]. The authors propose a few scoring functions to order the map landmarks according to their utility or to the observation statistics while guaranteeing a maximum coverage of the scene. An approach to map reduction was proposed in [26]. It aims to select only the places that are particularly suitable for localization using the *location utility* metric.

The remainder of this paper is organized as follows. First, we present an overview of our system. Next, we describe precisely our method for map summarization. Before concluding our work in the last section, experiments and results are presented for a small point cloud and then for a large-scale labelled point cloud.

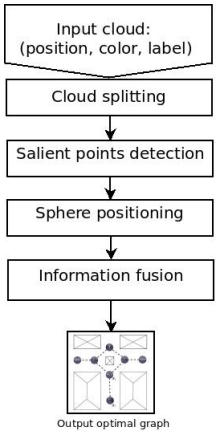

Fig. 1: Summarizing Large Scale 3D Point Cloud

III. OUR SOLUTION

Our work aims to perform several navigation tasks using only a map summary of the environment. This map should be not only compact but also coherent with the perception of the agent. To provide this map summary, we propose a new method dealing with large-scale 3D point clouds. The output of our summarizing method is a set of interconnected spherical images. Our main contributions are:

- We introduce the concept of *ViewPoint Entropy*, which is a measure of viewpoint's informativeness based on geometric, photometric and semantic characteristics. The ViewPoint Entropy is used to facilitate best viewpoint selection.
- Using *ViewPoint Entropy*, we formulate map summarizing process as an optimization problem.
- We propose a new representation of summarized localization map using augmented and labelled spherical images.
- We introduce a novel partitioning step in our scalable summarizing algorithm to allow large-scale point clouds handling.

In Fig. 1, we present the main steps of our algorithm to find the optimal set of spheres.

A. Cloud Splitting

To treat a large-scale 3D point cloud, we choosed to apply "Divide and Conquer" method. This algorithmic technique consists in:

- Divide : split an initial problem into sub-problems.
- Conquer : solve sub-problems recursively or directly if they are small enough.
- Combine : merge the solutions of the sub-problems to find the global solution of the initial problem.

In our case, we might manipulate a very large 3D cloud with high density of information representing a large part of an urban environment. This method is therefore the best-suited to our needs. The first step of our algorithm consists in splitting the large 3D cloud from the beginning into several subsets to determine the optimum position of the sphere representing each small region (subset). To do this, we have proposed a splitting method. This technique allows us to split the input cloud into several cells using a discrete set of points called "germs". These germs are the centers of the cells. To adequately split the input cloud, the centers must cover all the navigable areas in the cloud (zones of circulation for cars, bikes and pedestrians). To find the best set of centers, we randomly select several points from the cloud. A new point is added to the set of germs if it is far enough (about 3 or 4 meters in our case) from every one of them and it belongs to the navigable areas. This process will be repeated until there are no more points respecting the criteria of a germ. Fig. 2 shows an example of splitting a 3D point cloud.

Fig. 2: Splitting Large-scale point cloud

B. Salient Points Detection

In our final representation of the large-scale 3D point cloud, the salient areas must be represented in a very efficient way. To select these areas, we use the concept of visual saliency very commonly used these last years. There are many algorithms used for the detection of 3D visual saliency in a scene. Here, we consider three possible approaches dealing with saliency in 3D point cloud. They are based on the distinction between the regions in a scene. These methods are distinguished with the type of input information (geometric and photometric) used to extract salient points. The first method was proposed in [18]. This method uses a 3D point descriptor called Fast Point Feature Histogram (FPFH) (Geometric-based saliency) to characterize the geometry of the neighborhood of a point. A point is considered as distinct if its descriptor is dissimilar to all the other descriptors of points in the cloud. This operation is carried out on two levels with different neighborhood sizes. First, a low-level distinctness D_{low} is computed to detect the small features. Then, a value of association A_{low} is calculated to detect salient points in the neighborhood of the most distinct points. Next, a high-level distinctness D_{high} is computed to select the large features. The final saliency map is calculated for each 3D point p_i as follows:

$$S(p_i) = \frac{1}{2}(D_{low} + A_{low}) + \frac{1}{2}D_{high} \quad (1)$$

However, this method uses only the geometry of the scene without any other type of information such as colors. A new algorithm for detecting saliency in 3D point cloud was presented in a recent work [20] (Supervoxel-based saliency). This algorithm consists in exploiting the geometric features and the color characteristics together to estimate the saliency

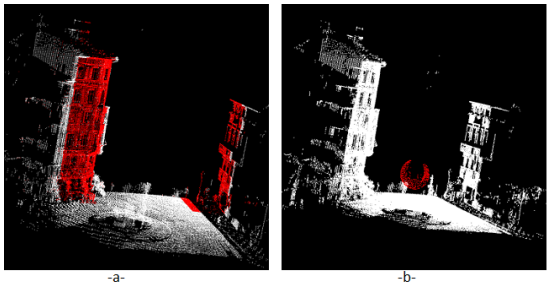

Fig. 3: Database (ground-truth) -a- manual segmentation -b- sphere positioning

in a cloud of colored points. All the 3D points are grouped in several supervoxels and then a measure of saliency for each set is calculated using the geometrical and photometric characteristics of its neighbors. This process is applied on several levels. Based on the center-surround contrast, a measure of the distinctness is computed for every cluster using its feature compared to each surrounding adjacent cluster's one. The feature contrast ρ_i of a given cluster *C* at a given level *i* is calculated as follows:

$$\rho_i(C) = \theta\rho_{geo}(C) + (1-\theta)\rho_{color}(C) \tag{2}$$

Where ρ_{geo} and ρ_{color} denote the normalized geometric and color feature contrast of the cluster *C*, and θ is a weighting parameter which is empirically set to 0.5 in [20]. Another method has been proposed in the work of Leroy [11] (Supervoxels-rarity) based only on supervoxels rarity. For each supervoxel v a measure of rarity $S_i(v)$ is calculated using only photometric characteristics (3).

$$S_i(v) = -log(P_i/N) \tag{3}$$

At each color component i, a self-information of the occurrence probabilities of the supervoxel P_i is obtained and N is the number of supervoxels. To evaluate the level of saliency captured by these methods, we have proposed to calculate a criterion called in the literature: F_β [12] . This criterion allows to characterize the relevance of the information returned by each method. This measure is calculated as follows:

$$F_\beta = \frac{(1+\beta^2) * (Precision * Recall)}{\beta^2 * Precision + Recall} \tag{4}$$

$$Recall = \frac{TP}{(TP+FN)} \tag{5}$$

$$Precision = \frac{TP}{(TP+FP)} \tag{6}$$

- True Positive (TP): number of points reasonably classified as relevant for localization
- False Positive (FP): number of points wrongly classified as relevant for localization
- False Negative (FN): number of points wrongly classified as irrelevant for localization

F_β score is the weighted harmonic mean of precision and recall and reaches its best value at 1 and worst score at 0.

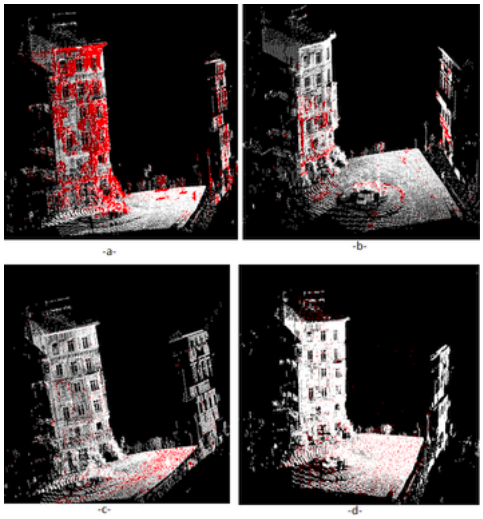

Fig. 4: Result of salient points detection according to the four 3D saliency extraction methods. -a- Geometric method [18] -b- Geometric and Photometric method [20] -c- Photometric method [11] -d- Harris3D [7]

Methods	F_β
Supervoxel-based saliency ($\theta = 0.7$) [20]	0.7401
Geometric-based saliency [18]	0.7234
Supervoxel-based saliency ($\theta = 0.5$) [20]	0.6696
Supervoxels-rarity [11]	0.5363
Harris3D [7]	0.4536

TABLE I: Results of salient points detection

Recall and precision are equally important if β is set to 1. $\beta < 1$ lends more weight to precision, while $\beta > 1$ favors recall. To contrast the approach of using the maximum recall of points (no discrimination) we decided that precision should be given much more priority over recall. In our work, β is set to 0.5 because it is one of the most common values assigned to β (recall is half as important as precision).

C. Sphere Positioning

After completing the decomposition of the initial problem (large size) into a set of sub-problems (small size), we search for the optimal position of the sphere in a 3D cloud using optimization methods. This problem is known as Optimal point of view selection. In this type of problem, we aim to determine the best possible location of the Viewpoint in order to maximize the amount of information given by this sphere center. In the next part, we consider the map-summarizing process as an optimization problem.

1) Problem Modeling: Our goal is to determine the best viewpoint allowing the capture of a maximum amount of salient points in the environment. This viewpoint will be represented by a spherical image. To find the optimal position of our sphere, we define a criterion called "Viewpoint Entropy". The output of the entropy optimization process is a 3D position (X_o, Y_o, Z_o) of the optimal sphere center. To select the most salient point for localization purpose, we propose to

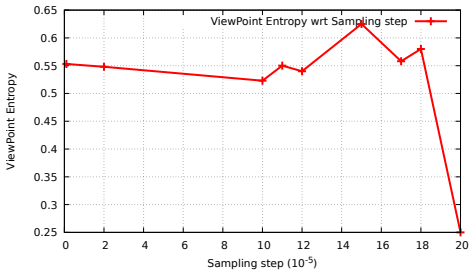

Fig. 5: Entropy value of a given dataset related to the sampling step

use photometric, geometric and semantic information of the studied environment. This criterion is defined below.

Entropy Calculation

We consider $\{P_i(X_i, Y_i, Z_i, R_i, G_i, B_i, L_i), i = 1..N\}$ as a finite set of N 3D points with their cartesian coordinates, their labels L_i and their colors (R_i, G_i, B_i), and a point $C(X_c, Y_c, Z_c)$ as the center of our sphere. The idea is to project all points of the cloud onto the sphere. For each point P_i, the coordinates (X, Y, Z) of the projected point on the sphere are:

$$\left(\frac{Xc + R(X_i - Xc)}{\|\vec{PC}\|}, \frac{Yc + R(Y_i - Yc)}{\|\vec{PC}\|}, \frac{Zc + R(Z_i - Zc)}{\|\vec{PC}\|} \right) \tag{7}$$

Subsequently, we make the conversion into spherical coordinates:

$$(\phi, \theta) = \begin{cases} \arccos(Z/\rho) \\ \arctan(Y/X) \end{cases} \tag{8}$$

R is the radius of the sphere (set to 1 in our work). The next step is to sample these projected points to have a homogeneous points ditribution on all the spheres. To do this, we use constant angle sampling. In the real-time implementation of on-line localization algorithms, this type of sampling methods was used in order to favor the calculation time [13]. This method consists in sampling the projected points on the sphere: P_s=(θ,ϕ), with angles $\theta \in [-\pi, \pi]$ and $\phi \in [0, \pi]$, using the sampling steps $\partial\theta$ et $\partial\phi$

$$\partial\theta = \frac{2\pi}{m}, \partial\phi = \frac{\pi}{n} \tag{9}$$

In this equation *m* denotes the number of samples in latitude and *n* the number of samples in longitude. We conducted a small study of the influence of the sampling step on the entropy value, regardless of other factors, on a given test dataset containing 60,000 3D points and representing an urban environment. The results are shown on Fig. 5. It appears that it decreases strongly for values above 15 x 10^{-5} rad. However, smaller values will increase the data volume thus we recommend staying with that value.

To obtain the corresponding intensity for each projected pixel, an interpolation is applied using the intensity of the nearest neighbor. We propose to define two levels of saliency in a 3D point cloud. The low-level saliency S^{low} is based on low-level characteristics (photometric and geometric) of a 3D point. The high-level saliency S^{high} is based on the semantic information of each 3D point. To compute S^{low} values we use the Supervoxel-based saliency method described in the previous section which allows the combination of photometric and geometric information. We have chosen this method because it ensures a compromise between the calculation time and the selection of the most salient points useful for the localization. To compute S^{high} values, we use the semantic Labels for each point. Using these two types of saliency, we calculate the number of points of interest on the sphere according to their relevance. Therefore, we have four possible combinations as following.

- n_{00}: number of non relevant points semantically, photometrically and geometrically.
- n_{10}: number of points relevant only photometrically and geometrically.
- n_{01}: number of points relevant only semantically.
- n_{11}: number of points relevant semantically, photometrically and geometrically.

The entropy of a sphere will be characterized by the entropy of its center P. The entropy is given by the algorithm 15:

Algorithm 1 Entropy

Input : $\{P_j(X_j, Y_j, Z_j, S_j^{low}, S_j^{high}) \in S, j = 1..M\}$ ▷ M is the number of projected points on the sphere S of center C
Output : $\xi(C) \in [0..1]$

procedure $\xi(C)$ ▷ The entropy of the center C
  $\xi(C) \leftarrow 0$
  $j \leftarrow 1$
  $n_{00} \leftarrow 0, n_{01} \leftarrow 0, n_{10} \leftarrow 0, n_{11} \leftarrow 0$
  for $j = 1$ to M **do**
    if $((S_j^{low} = 0) and (S_j^{high} = 0))$ **then**
      $n_{00} \leftarrow n_{00} + 1$
    else if $((S_j^{low} = 1) and (S_j^{high} = 0))$ **then**
      $n_{10} \leftarrow n_{10} + 1$
    else if $((S_j^{low} = 0) and (S_j^{high} = 1))$ **then**
      $n_{01} \leftarrow n_{01} + 1$
    else
      $n_{11} \leftarrow n_{11} + 1$
    end if
  end for
  $\xi(C) \leftarrow$
$-\frac{n_{00}}{M} \log \frac{n_{00}}{M} - \frac{n_{01}}{M} \log \frac{n_{01}}{M} - \frac{n_{10}}{M} \log \frac{n_{10}}{M} - \frac{n_{11}}{M} \log \frac{n_{11}}{M}$
  return $\xi(C)$
end procedure

2) Optimization: The Best Viewpoint Selection is an entropy optimization process. This optimal point of view is the center of our optimal sphere. To maximize the entropy criterion, we have proposed a genetic algorithm to determine the maximum of entropy function $\xi : X \rightarrow \mathbf{R^3}$, where X is the initial population of *N* 3D points. These points are the centers of the spheres on a navigable area in the cloud. This

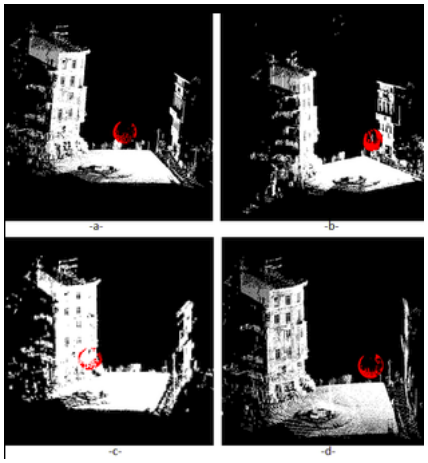

Fig. 6: Result of spheres positioning according to the four 3D saliency extraction methods. -a- Geometric method [18] -b- Geometric and Photometric method [20] -c- Photometric method [11] -d- Harris3D [7]

optimization algorithm consists in evaluating the entropy of each member in the population. Both individuals (parents) with maximum entropy values are selected. The combination of two parents in a first iteration allows us to obtain a solution (child) with a better entropy than these parents. Thanks to this evolution of the viewpoint selection from one iteration to another, the algorithm becomes able to converge towards a solution among the points maximizing the entropy after a few iterations. The optimization algorithm is defined as follows:

Algorithm 2 Genetic Algorithm

Inputs : Navigable area $\{P_i(X_j, Y_j, Z_j) \in Z, i = 1..N\}$ Number of iterations N_{iter} Number of individuals N_{indiv}
Output : Best viewpoint $V \in Z$

procedure $GA(Z)$
  $k \leftarrow 1$
  $I \leftarrow$Select N_{indiv} random points $\in Z$
  while $k < N_{iter}$ **do**
    for each point p_h in I **do** $entropy(h) \leftarrow \xi(p_h)$
    end for
    $parent1 \leftarrow arg\,max_1(entropy)$
    $parent2 \leftarrow arg\,max_2(entropy)$
    for $l = 1$ to N_{indiv} **do**
      Add $\lambda * parent1 + \alpha * parent2$ To I
        ▷ λ and α random numbers $\in [0..1]$
    end for
  end while
  return $(arg\,max(entropy))$
end procedure

This algorithm has two parameters: maximum number of iterations N_{iter} and initial population size N_{indiv}). To be able to assign a value to them and maintaining a reasonnable computing time, we conducted a small study on some sample dataset of 30 000 points. To find the optimal value of N_{indiv},

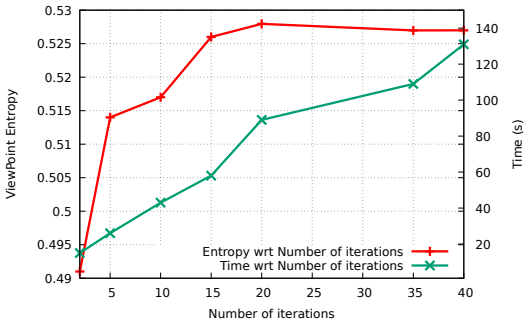

(a) Number of iterations

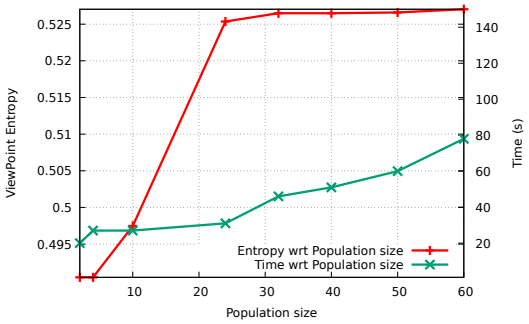

(b) Population size

Fig. 7: Entropy and computation time values of a given dataset related to the population size and the number of iterations

we set N_{iter} to 5 and we measure the computation time and the entropy value while varying N_{indiv}. Results can be seen on Fig. 7a and show that values of N_{indiv} above 20 give the best results. However, higher values also increase computation time. Similarly, Fig. 7b shows the he entropy value when N_{iter} varies while fixing $N_{indiv} = 20$. It shows that values of N_{iter} above 15 are sufficient to reach a compromise between the algorithm convergence and the computation time.

D. Information Fusion

After the splitting and the sphere positioning steps, we will present, in this section, the last step of our algorithm allowing the calculation of the similarity between the obtained spheres. Then, the similar spheres are merged to eliminate the redundant information. This correlation (similarity) expresses the variation rate of the photometric, semantic and geometric information between every two compared spheres. In Meilland's work [14], this criterion is calculated using the Median Absolute Deviation (MAD) which represents the difference (error) of intensity between the pixels of the two spheres (compared pixel by pixel). Similarly, we have proposed to add a measure of semantic similarity S_{sem} between two spheres. This measure aims to compute the number of similar pixels having the same label. We have also added a measure of geometric similarity by computing a histogram using the geometric descriptor FPFH. By comparing the histograms of different spheres we have obtained a measure of geometric

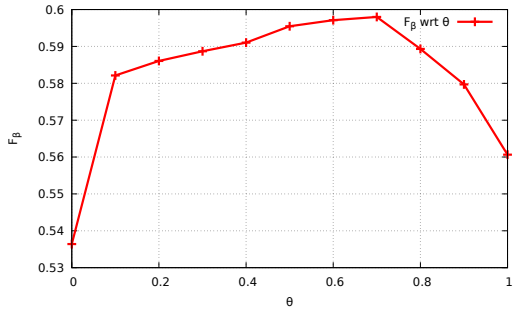

Fig. 8: Evolution of F_β of a given dataset related to the mixing parameter θ

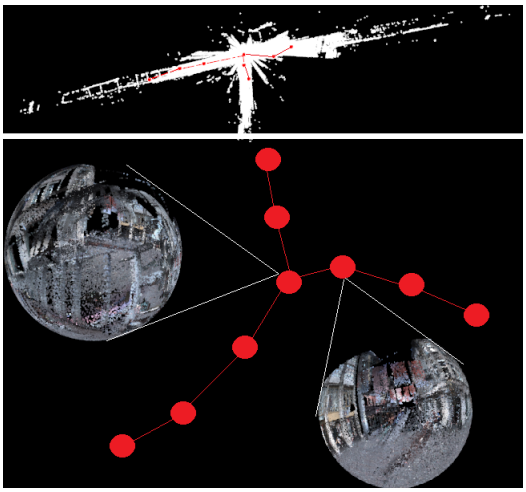

Fig. 9: 3D point cloud Summary

similarity S_{geom}.

$$\begin{aligned} S_{phot} &= \text{med}(|p(x) - \text{med}(p(x))|) \\ S_{sem} &= \text{med}(|s(x) - \text{med}(s(x))|) \\ S_{geom} &= \text{med}(|g(x) - \text{med}(g(x))|) \\ S &= mean(S_{phot} + S_{geom} + S_{sem}) \end{aligned} \tag{10}$$

In this equations, $p(x), s(x)$ and $g(x)$ are respectively the vectors containing the photometric, semantic and geometric errors between the pixels of the two spheres. Theoretically, two or more spheres are considered similar if the S value is lower than a certain threshold. This is due to the small distance between the spheres. If two or more spheres are similar, a merging process is launched. This process consists in concatenating the two or more corresponding regions to the compared spheres and then re-applying the optimization method (Genetic Algorithm) in order to merge the similar spheres into one representing all the regions.

IV. Results

A. Small 3D Point Cloud

At the beginning, we have tested our algorithm on a first database containing 60,000 3D points [21]. This point cloud, developped originally without semantic information, represents an urban environment and covers around 400 m^2. We have used this dataset to compare the 3D Saliency Extraction methods and to verify the estimated location of the optimal sphere. Because of its small size, this dataset is considered as a sub-part of a larger point cloud. Therefore, it was not necessary to apply the splitting step. We have chosen to implement and test the three methods detailed in the second section and the Harris3D [7] to extract a saliency map. We have compared the 3 methods, as detailed in the previous section, and also the method of interest points detector Harris3D known for its simplicity and efficiency in computer vision applications.

In order to build a ground-truth map before comparing these methods, we have manually segmented this urban database by choosing the most salient and useful points for localization. Among these points, we have selected those belonging to the building facade (front), the road signs and the ground marking. This ground-truth allowed the evaluation of the obtained results. Fig. 4 shows the result obtained by each method. Table I shows the F_β values obtained by the four methods. The two algorithms using geometry to compute the saliency map had given better results than methods using only photometry because, in our case, points of interest for localization are generally more salient geometrically than photometrically. Fig. 6 shows the result of positioning the sphere in this scene. These results are obtained using a genetic algorithm for entropy optimization. We have obtained four results in the form of a position (x, y, z) of the center of the sphere summarizing the scene. Fig. 3 shows our ground truth. The sphere of the ground-truth is computed using the optimization algorithm (GA) and the ground-truth saliency map as described above. This sphere is located at equi-distance of the buildings and we have judged it to be the best point of view to visualize all the points of interest in this scene. We have calculated euclidean distance between the resulting spheres of the four methods and the sphere of the ground-truth (table I) to determine which one is the closest to the ground-truth sphere. The results obtained with the methods using geometry are the closest to the ground truth. We have obtained a compression ratio around 87%.

B. Large-Scale 3D Point Cloud

In the next part of our work, we have applied our method on a much larger environment. This large-scale point cloud contains over 40 millions of 3D labelled points [8]. In this dataset, we have 8 classes of labels (Fig. 10), namely {1: man-made terrain, 2: natural terrain, 3: high vegetation, 4: low vegetation, 5: buildings, 6: hard scape, 7: scanning artefacts, 8: cars}. An additional label {0: unlabeled points} marks points without any semantic value. In our summarizing process, points labelled "buildings", are considered among the most salient points for localization. This dataset permitted the evaluation of our solution's performance by using all semantic, photometric and geometric characteristics together. After splitting this large-scale point cloud, we have obtained 72 sub-clouds. To compute the saliency map we have chosen

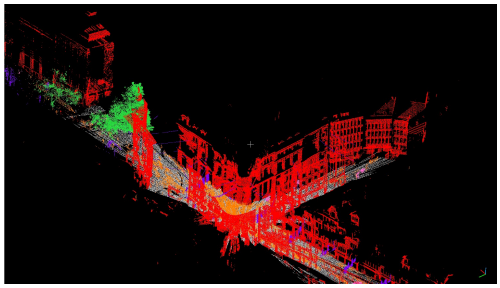

Fig. 10: Semantic 3D Large-scale point cloud

the second method seeing that it provides a compromise between the relevance of the result and the time consumption. The parameter θ in equation 2 that controls the preference between geometric and photometric distinctness is assigned to a value of 0.7. This value has been chosen after a short study of the influence of the mixing parameter θ on the entropy value, on a small 3D Point Cloud described in the previous section. The results can be seen on Fig. 8 and clearly justify this value.

The output of this summary process, as shown in the Fig. 9, is a compact set of spherical images. We have obtained 35 spheres summarizing a point cloud of about 160 m length. The mean distance between all the spheres is around 4.5 m. We have obtained a good compression ratio of this map (93%). To evaluate our solution, we have computed Recall and Precision (equations 5 and 6). They are defined as follows :

- True Positive (TP): number of relevant points actually projected on the spheres
- False Positive (FP): number of irrelevant points actually projected on the spheres
- True Negative (TN): number of irrelevant and non-projected points on the spheres
- False Negative (FN): number of relevant and non-projected points on the spheres

We have built our ground truth dataset. For each point in the cloud, we have attributed a label $\{0$: irrelevant for localization, 1 : relevant for localization$\}$. Most of the relevant points belong to buildings thanks to their geometric shapes. As a result, we have significantly decreased the size of the map. Nevertheless, we have succeded to keep a maximum number of salient points (Recall around 60%) with a good level of precision (greater than 91 %). To improve the recall value, we could refine the input semantic labels to select the finest and most useful areas for localization (windows, doors, panels ...). All the spheres are positioned in a way to capture the maximum possible points belonging to the front facades of the buildings.

V. CONCLUSIONS

The developped method throughout this project allows us to summarize efficiently a large-scale point cloud. The summarizing process is based on the extraction of several spherical view representing sub-clouds of the initial map. This spherical representation contains semantic, photometric and geometric information. This new method of summarizing 3D maps will allow us to facilitate several navigation tasks when applied in intelligent transportation systems (localization, route planning, obstacle avoidance, ...) by reducing significantly the calculation time and the memory size required to the functioning of the navigation systems. We also believe that using the semantic information permits the development of a precise summary map by rejecting unnecessary localization data such us points belonging to dynamic objects (cars, pedestrians...). Thanks to "divide and conquer" technique, we have proposed a scalable summarizing algorithm dealing with large-scale point clouds. Our method outperforms existing systems. It enables the compressing of a 30,000 points cloud in less than 1 minute compared to 30 minutes as mentioned in [27]. In our future works, we will aim to provide a multilevel map in which a special level will be fully dedicated to every transportation system (trains, cars, bikes, pedestrians...) to enhance the navigation precision.

VI. ACKNOWLEDGMENTS

This work takes part in the ANR-15-CE23-0010-01 pLaTINUM project. This project has been funded with the support from the French National Research Agency (NRA).

REFERENCES

[1] Jae-Kyun Ahn, Kyu-Yul Lee, Jae-Young Sim, and Chang-Su Kim. Large-scale 3d point cloud compression using adaptive radial distance prediction in hybrid coordinate domains. *IEEE Journal of Selected Topics in Signal Processing*, 9(3):422–434, 2015.

[2] Selim Benhimane, Alexander Ladikos, Vincent Lepetit, and Nassir Navab. Linear and quadratic subsets for template-based tracking. In *IEEE Conference on Computer Vision and Pattern Recognition*, pages 1–6, 2007.

[3] Dana Cobzas, Hong Zhang, and Martin Jagersand. Image-based localization with depth-enhanced image map. In *Robotics and Automation*, volume 2, pages 1570–1575, 2003.

[4] Olivier Devillers and P-M Gandoin. Geometric compression for interactive transmission. In *Visualization 2000. Proceedings*, pages 319–326. IEEE, 2000.

[5] Gabriela Gallegos, Maxime Meilland, Patrick Rives, and Andrew I Comport. Appearance-based slam relying on a hybrid laser/omnidirectional sensor. In *Intelligent Robots and Systems (IROS)*, pages 3005–3010, 2010.

[6] Pierre-Marie Gandoin and Olivier Devillers. Progressive lossless compression of arbitrary simplicial complexes. *ACM Transactions on Graphics (TOG)*, 21(3):372–379, 2002.

[7] Chris Harris and Mike Stephens. A combined corner and edge detector. In *Alvey vision conference*, volume 15, page 50, 1988.

[8] IGP and CVG. Large-Scale Point Cloud Classification. Benchmark. http://www.semantic3d.net/, 2016.

[9] Matjaz Jogan and Ales Leonardis. Robust localization using panoramic view-based recognition. In *Pattern Recognition*, volume 4, pages 136–139, 2000.

[10] Julius Kammerl, Nico Blodow, Radu Bogdan Rusu, Suat Gedikli, Michael Beetz, and Eckehard Steinbach. Real-time compression of point cloud streams. In *Robotics and Automation (ICRA), 2012 IEEE International Conference on*, pages 778–785, 2012.

[11] Julien Leroy, Nicolas Riche, Matei Mancas, and Bernard Gosselin. 3d saliency based on supervoxels rarity in point clouds.

[12] Ran Margolin, Lihi Zelnik-Manor, and Ayellet Tal. How to evaluate foreground maps? In *IEEE Conference on Computer Vision and Pattern Recognition*, pages 248–255, 2014.

[13] Maxime Meilland, Andrew I Comport, and Patrick Rives. A spherical robot-centered representation for urban navigation. In *Intelligent Robots and Systems (IROS)*, pages 5196–5201, 2010.

[14] Maxime Meilland, Andrew I Comport, and Patrick Rives. Dense omnidirectional RGB-D mapping of large-scale outdoor environments for real-time localization and autonomous navigation. *Journal of Field Robotics*, 32(4):474–503, 2015.

[15] Emanuele Menegatti, Takeshi Maeda, and Hiroshi Ishiguro. Image-based memory for robot navigation using properties of omnidirectional images. *Robotics and Autonomous Systems*, 47(4):251–267, 2004.

[16] Anthony Remazeilles, François Chaumette, and Patrick Gros. Robot motion control from a visual memory. In *Robotics and Automation*, volume 5, pages 4695–4700, 2004.

[17] Ruwen Schnabel and Reinhard Klein. Octree-based point-cloud compression. In *Spbg*, pages 111–120, 2006.

[18] Elizabeth Shtrom, George Leifman, and Ayellet Tal. Saliency detection in large point sets. In *IEEE International Conference on Computer Vision*, pages 3591–3598, 2013.

[19] Fraundorfer, Friedrich and Engels, Christopher and Nistér, David. Topological mapping, localization and navigation using image collections. *IROS*, 3872–3877, 2007.

[20] Jae-Seong Yun and Jae-Young Sim. Supervoxel-based saliency detection for large-scale colored 3d point clouds. In *IEEE International Conference (ICIP)*, pages 4062–4066, 2016.

[21] Bernhard Zeisl, Kevin Koser, and Marc Pollefeys. Automatic registration of rgb-d scans via salient directions. In *international conference on computer vision*, pages 2808–2815, 2013.

[22] Whitley, L Darrell Foundations of genetic algorithms. *morgan Kaufmann*, 1993.

[23] Marcin Dymczyk, Simon Lynen, Titus Cieslewski, Michael Bosse, Roland Siegwart, and Paul Furgale The gist of maps-summarizing experience for lifelong localization *Robotics and Automation* , 2015.

[24] Muhlfellner, P., Burki, M., Bosse, M., Derendarz, W., Philippsen, R., Furgale Summary maps for lifelong visual localization *Journal of Field Robotics* , 2015.

[25] Hyun Soo Park, Yu Wang, Eriko Nurvitadhi, James C Hoe, Yaser Sheikh, and Mei Chen 3d point cloud reduction using mixed-integer quadratic programming *Computer Vision and Pattern Recognition Workshops* , 2013

[26] Ted J. Steiner, Guoquan Huang, and John J. Leonard Location utility-based map reduction *obotics and Automation* , 2015

[27] H. S. Park, Y. Wang, E. Nurvitadhi, J. Hoe, Y. Sheikh, and M. Chen, 3d point cloud reduction using mixed-integer quadratic programming *Computer Vision and Pattern Recognition Workshops (CVPRW)* , 2013